Thermal Tuning of High-Tc Superconducting Bi2Sr2CaCu2O8+δ Terahertz Metamaterial

Thermal Tuning of High-T_c Superconducting Bi$_2$Sr$_2$CaCu$_2$O$_{8+\delta}$ Terahertz Metamaterial

S. Kalhor
M. Ghanaatshoar
T. Kashiwagi
K. Kadowaki, *Member, IEEE*
M. J. Kelly, *Senior Member, IEEE*
K. Delfanazari, *Member, IEEE*
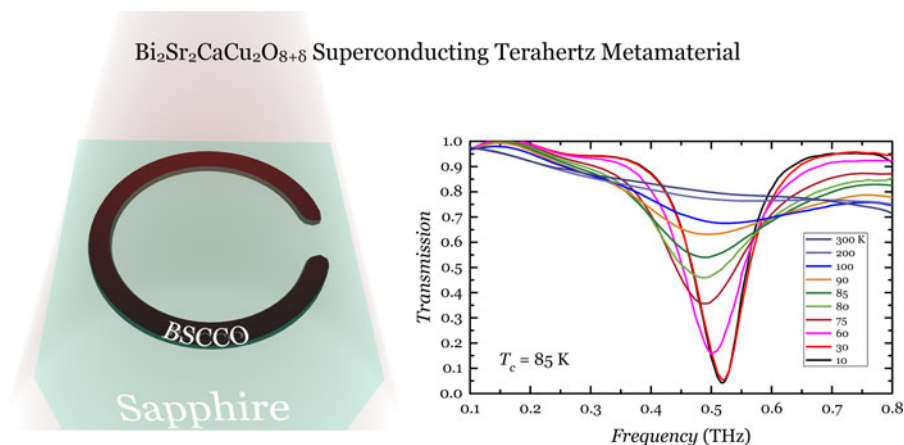
Bi$_2$Sr$_2$CaCu$_2$O$_{8+\delta}$ Superconducting Terahertz Metamaterial

Thermal Tuning of High-T_c Superconducting Bi$_2$Sr$_2$CaCu$_2$O$_{8+\delta}$ Terahertz Metamaterial

S. Kalhor,[1] M. Ghanaatshoar,[1] T. Kashiwagi,[2,3]
K. Kadowaki,[2,3] *Member, IEEE*, M. J. Kelly,[4,5] *Senior Member, IEEE*,
and K. Delfanazari ,[4,5] *Member, IEEE*

[1]Laser and Plasma Research Institute, Shahid Beheshti University, G.C., Evin, 1983969411, Tehran, Iran
[2]Graduate School of Pure and Applied Sciences, University of Tsukuba, 1-1-1 Tennodai, Tsukuba, Ibaraki 305-8571, Japan
[3]Division of Material Sciences, Faculty of Pure and Applied Sciences, University of Tsukuba, 1-1-1 Tennodai, Tsukuba, Ibaraki, 305-8573, Japan
[4]Department of Physics, Cavendish Laboratory, University of Cambridge, Cambridge CB3 0HE, U.K.
[5]Centre for Advanced Photonics and Electronics, Electrical Engineering Division, University of Cambridge, Cambridge CB3 0FA, U.K.

Abstract: We introduce a class of low-loss subwavelength resonators and report the first demonstration of a high-temperature (T_c) superconducting Bi$_2$Sr$_2$CaCu$_2$O$_{8+\delta}$ (BSCCO) terahertz (THz) metamaterial. The numerical simulations and analytical calculations are performed to study the electromagnetic response of the subwavelength BSCCO split-ring resonators (SRRs) to the incident photons with energies below the superconducting gap energy. A transition of resonance strength is observed as a dip in resonance frequency for temperatures below BSCCO T_c. To interpret the transmission spectra, resonance switching, and frequency tuning of SRRs, we calculate the temperature dependent complex permittivity and surface impedance of a 200 nm thick unpatterned slightly underdoped BSCCO thin film. We compare the resonance tunability of SRRs made of the extremely disorder superconductor (BSCCO) with metamaterials made of a weakly disorder superconductor YBa$_2$Cu$_3$O$_7$ (YBCO) and show that the resonance quality and frequency tuning are comparable for these two metamaterials. Our results may be useful for THz emitters and detectors developments, for instance, by integration of SRRs with BSCCO THz emitters and microstrip antennas, the device functionalities such as polarization, emission pattern directivity, and output power could be controlled and improved.

Index Terms: Antennas and split-ring resonators, BSCCO THz emitters and detectors, superconducting metamaterials.

1. Introduction

The electromagnetic response of superconductors is derived from Cooper pairs which is very sensitive to external perturbations such as induced current, magnetic field, light photons, and temperature [1]. Among superconducting materials, the anisotropic layered high-T_c superconductors
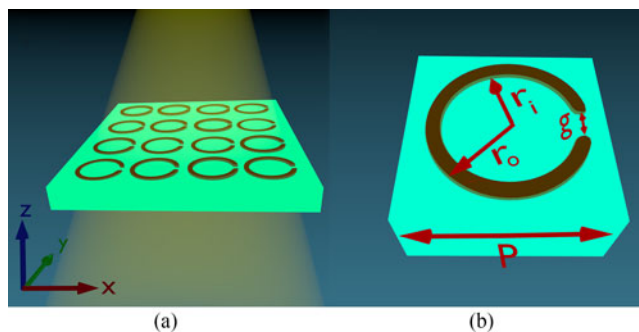
Fig. 1. a) The schematic diagram of the proposed BSCCO THz metamaterial on the sapphire substrate under normal illumination. BSCCO SRRs are shown in dark-brown and sapphire substrate is depicted in cyan. b) BSCCO meta-atom unit cell with structural parameters: $g = 1$ μm, $r_o = 40$ μm, $r_i = 35$ μm and $P = 90$ μm.

that are composed of alternating metallic (and superconducting below T_c) CuO_2 and insulating double layers, are intrinsically left-handed materials, showing the existence of surface Josephson plasma waves [2], and realizing negative refractive index metamaterials [3]. With these advantages, together with their high T_c, they have received attention in optics and photonics: the extraordinary transmission [4], [5], Fano resonances [6], nonlinear metamaterial [7] and saturable absorbers [8] have been recently reported with metamaterials made of YBCO superconductor operating at sub-THz and THz frequencies.

However, YBCO is a superconductor with relatively weak anisotropy, which has a small damping rate and remarkably sharp plasma resonance [9], [10]. Until now, split-ring resonators (SRRs) metamaterials made of superconductors with extreme anisotropy such as BSCCO layered high-T_c superconductors have not been reported. BSCCO with large superconducting energy gap (up to 60 meV) [11] exhibits fascinating electromagnetic responses, for example, it is the building block of a solid state, compact, powerful, continuous and coherent THz wave emitters and detectors [11]–[19]. To have a commercial superconducting BSCCO THz emitter useful in most applications some of their functionalities such as emission polarization, directivity, and output power should be efficiently controlled and developed. Among BSCCO films of various carrier concentrations (doping) the slightly underdoped film is preferred in fabrication of such emitters because the emission of THz radiation takes place in the resistive state of the current-voltage characteristic (IVCs), so the critical current-normal resistance product ($I_c R_N$) should be as high as possible [20], [21].

In this paper, we propose a class of low-loss SRRs array based on BSCCO superconductor. We discuss the temperature (T) dependent complex permittivity and surface impedance of a 200 nm thick unpatterned slightly underdoped BSCCO thin film ($T_c = 85$ K) and utilize the numerical simulation and analytical calculations to study the resonance frequency and transmission amplitude tuning of BSCCO SRRs at THz frequencies and T ranges of 10-300 K. We show that our numerical simulations of the T-dependent metamaterial resonance switching and frequency tuning are well reproduced with theoretical calculations.

2. Results and Discussion

The schematic diagram of the proposed THz BSCCO SRRs array under the normal incident illumination with respect to the metamaterial plane is shown in Fig. 1(a). We numerically simulate the electromagnetic (EM) response of the metamaterial by using 3D EM solver COMSOL Multiphysics. In simulation, to get the highest possible resonance quality from the subwavelength BSCCO SRRs, we chose thickness $d = 200$ nm, the inner- $r_i = 35$ μm and outer-radius $r_o = 40$ μm, ring gap size $g = 1$ μm and the unit cell periodicity $P = 90$ μm (see Fig. 1(b)). A 500 μm thick sapphire plate is chosen as the substrate. The superconducting BSCCO metamaterial can be fabricated by either photography or focus ion beam (FIB) milling.
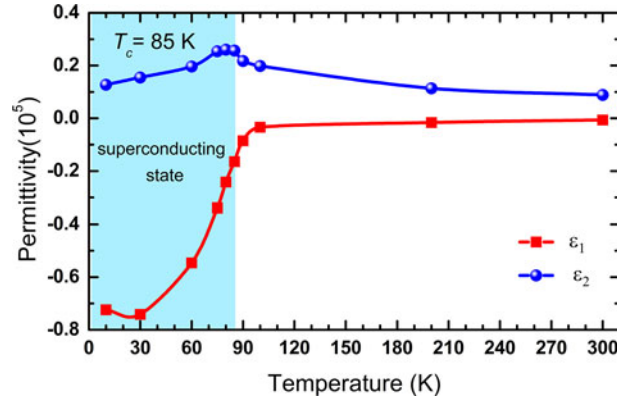
Fig. 2. The temperature dependence complex permittivity of slightly underdoped BSCCO thin film at $f = 0.5$ THz extracted from the THz-TDS measurements.

The complex $a-b$ plane conductivity $\sigma_1 + i\sigma_2$ of MBE-grown BSCCO thin film [22] is extracted from the terahertz time-domain spectroscopy (THz-TDS) experiment where the electric field of the illuminated EM wave was parallel to the BSCCO $a-b$ plane [23]. The anisotropy within $a-b$ plane was neglected. BSCCO is a highly anisotropic material [24], [25] with anisotropy parameter $\lambda_c/\lambda_{ab} > 100$ which λ_c and λ_{ab} are magnetic penetration depth along the c-axis and $a-b$ planes respectively [26]. The penetration depth is inversely proportional to the square root of conductivity [27] so conductivity is larger along the $a-b$ plane that contains the c-axis plasma frequency [9].

In Fig. 2, we plotted the calculated T-dependent complex $a-b$ plane permittivity of slightly under-doped BSCCO thin film at frequency $f = 0.5$ THz and magnetic field $B = 0$ T. We are particularly interested in this frequency because it is in the middle of the frequency range that contains both the c-axis plasma frequency and the quasiparticle scattering rates in the superconducting state of BSCCO. The complex permittivity is calculated from the experimental complex conductivity using the relation [28]:

$$\varepsilon = \varepsilon_1 + i\varepsilon_2 = (\varepsilon_\infty - \sigma_2/\omega\varepsilon_0) + i(\sigma_1/\omega\varepsilon_0) \tag{1}$$

where ω is angular frequency, ε_0 and ε_∞ are the dielectric constant of vacuum and optical dielectric constant, respectively. The ε_∞ affects the real part of permittivity only with no major effect below 30 THz [29].

The two-fluid model is widely used to explain the conductivity of YBCO in microwave, THz and infrared frequencies [4], [6], [8]. The scattered quasiparticles due to thermally generated plasmons (therefore large $1/\tau$ in the superconducting state) results in the failure of this model in BSCCO in microwave and millimeter waves regime. For $f < 150$ GHz, the T-dependent real conductivity is frequency independent and only above this frequency we can see the change in σ_1 [9]. In BSCCO, about one-third of the quasiparticle spectral weight remains uncondensed even when T approaches to 0 K, therefore a modified two-fluid model with an additional contribution to $\sigma_1(T)$ beyond the Drude response of quasiparticles -as the collective component- is needed to explain the optical properties of the material [23]. By including the collective contribution into the real conductivity, we will have:

$$\sigma_1(T, \omega) = \frac{\rho_n\tau}{1 + \omega^2\tau^2} + \frac{\kappa\rho_s/\Gamma_{cm}}{1 + \omega^2/\Gamma_{cm}^2} \tag{2}$$

where, $\rho_n(T) + \rho_s(T) = \rho_s(0)$ [30].

Here, ρ_n, ρ_s, κ, and Γ_{cm} are the normal and superfluid densities, the T-independent fraction of $\rho_s(0)$ that remains uncondensed at $T = 0$ K, and the width of the uncondensed contribution, respectively.

The first term in (2) describes the Drude contribution from condensed quasiparticles and the second term explains a Lorentzian peak which models the collective mode [9], [23] [30].
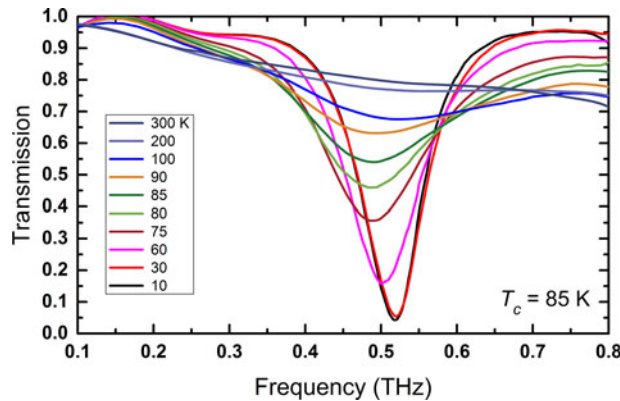
Fig. 3. The frequency dependence THz transmission amplitude spectra of an array of slightly under-doped BSCCO SRRs at various temperatures.

The real conductivity (or imaginary permittivity ε_2 in Fig. 2) of BSCCO derived from (2) increases by decreasing T and shows a crossover at $T = 80$ K, close to T_c. Although it will decrease when material enters the superconducting state but the value at lowest temperature 5 K is comparable to $T = 300$ K. This behavior suggests that although $\rho_s(T)$ increases linearly with decreasing T, it is compensated by significantly large scattered quasiparticles due to thermally generated plasmons [9], [23], [30].

$$\sigma_2(T, \omega) = \frac{\rho_n \omega \tau^2}{1 + \omega^2 \tau^2} + \frac{\rho_s}{\omega} \tag{3}$$

The imaginary conductivity (or real permittivity ε_1 in Fig. 2) of BSCCO derived from (3) is almost constant by decreasing T from 300 K down to T_c due to the absence of ρ_s in this region. By further reducing T and entering the superconducting state, the ratio of ρ_s to ρ_n increases. This results in the significant change in imaginary conductivity of the BSCCO below T_c.

The simulated frequency dependent transmission amplitude spectra of the slightly underdoped BSCCO SRRs for incident light with electric field E parallel to the SRRs gap are shown in Fig. 3 at various temperatures. In our simulation, the transmission spectra of all temperatures are normalized to the transmission spectra of a bare sapphire [31] to eliminate the substrate response. we used the periodic boundary condition in the lateral directions of a unit cell to approximate the transmission of an infinite number of SRRs.

As shown in Fig. 3, the transmission spectra of SRRs have the strongest resonance response at 10 K (far below T_c) as indicated by a sharp dip at 0.52 THz (black curve) with a minimum value of 0.051. As the temperature increases, the resonance strength decreases resulting in broadening and amplitude reduction of the transmission dip. The response completely vanishes at $T > 100$ K.

The resonance frequency experiences a red-shift that reaches the lowest value of 0.49 THz as T is raised to 85 K. By further increasing T, the resonance frequency retunes back to higher frequencies but the resonance strength continues to decrease.

The applied incident field excites circulating current in the SRRs [32] as shown in Fig. 4(a). The induced current in the SRRs accumulate at gap edges and therefore the electric field enhances across the capacitive gap. The electric field distribution is shown in Fig. 4(b). The induced circulating current induces a magnetic field with its maximum magnitude around the inner and outer parts of the SRR. The z-component of the magnetic field is shown in Fig. 4(c).

The red curve in Fig. 5 shows the simulated transmission minimum at resonance frequencies of the SRRs. We see that the transmission minimum increases sharply by increasing T until it saturates above T_c. The thermally tuned resonance response of our metamaterial can be interpreted by studying the T-dependent resistance and inductance of the slightly underdoped superconducting BSCCO thin film.
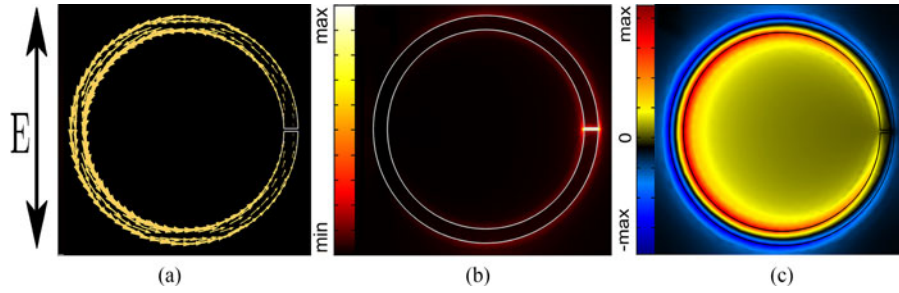
Fig. 4. (a) The excited circulating currents, (b) the electric field distribution, and (c) the induced z-component of the magnetic field for slightly underdoped BSCCO SRRs at 10 K. The polarization of the incident light is indicated as parallel to the gap direction.
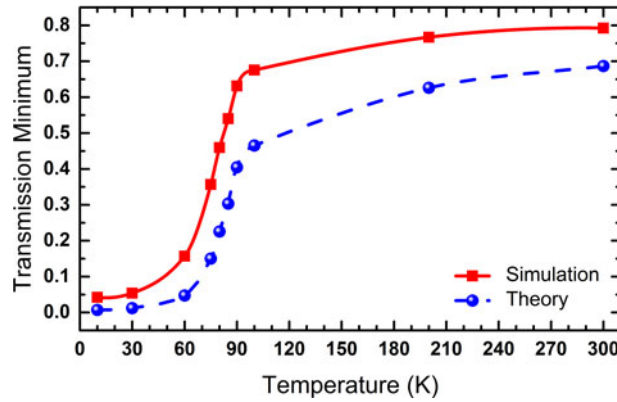

Fig. 5. The temperature dependent transmission minimum of the slightly underdoped BSCCO SRRs. The red solid line is the simulation result while the blue broken line is calculated from (9).

The complex surface impedance Z_s of an unpatterned BSCCO conducting thin film can be calculated from the equation:

$$Z_s = R_s - iX_s \cong \sqrt{i\omega\mu_0/2\sigma} \cot(\sqrt{i\omega\mu_0\sigma}d) \qquad (4)$$

where d is the thin film thickness and μ_0 is the permeability of vacuum [33]. This equation shows that both the real and imaginary conductivities contribute to the BSCCO surface impedance. The calculated surface resistance R_s (red) and the surface reactance X_s (blue) of slightly underdoped BSCCO are plotted at $f = 0.5$ THz in Fig. 6(a). The R_s determines the strength of the resonance. By increasing T, the R_s increases, therefore the resonance linewidth becomes broader and the transmission minimum increases (see the red solid line in Fig. 5).

The superconducting inductance L_s and the resistance R of a BSCCO SRR was obtained from the impedance of the superconducting thin film [34]:

$$L_s = \frac{X_s}{\omega} \frac{2\pi r - g}{w} \qquad (5)$$

$$R = R_s \frac{2\pi r - g}{w} \qquad (6)$$

with

$$w = r_o - r_i, \qquad (7)$$
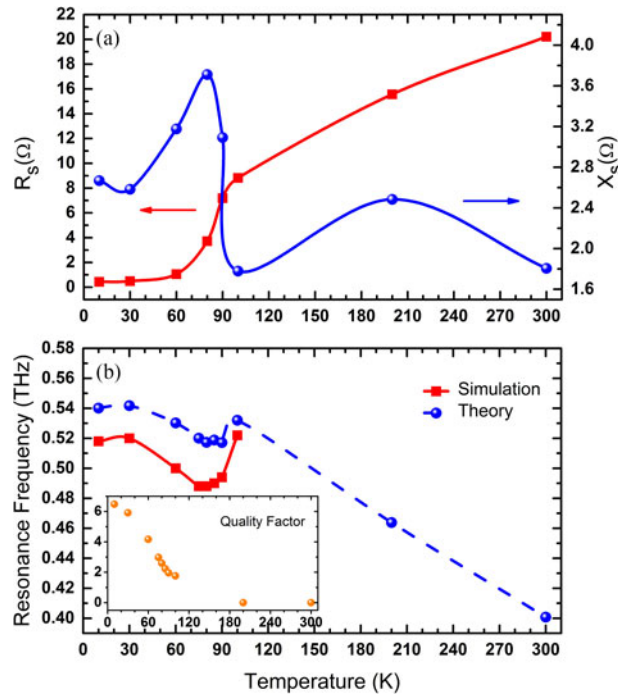
$$r = r_i + w/2 \qquad (8)$$

Fig. 6. (a) The T-dependent surface resistance R_S and reactance X_S of a slightly underdoped BSCCO thin film at 0.50 THz. (b) The temperature dependent resonance frequency of the slightly underdoped BSCCO SRRs. The red solid line is the simulation result while the blue broken line is calculated from (10). The inset is temperature dependent resonance quality factor.

The theoretical minimum transmission at resonance frequency can be calculated from:

$$T = \left(\frac{1 + n_s}{1 + n_s + Z_0/R} \right)^2 \tag{9}$$

where n_s is the refractive index of sapphire and Z_0 is the impedance of vacuum [33].

The minimum transmission calculated from (9) is plotted in Fig. 5 in blue Broken line. We see that the calculations are consistent with numerically simulated results. In both cases, the transmission minimum increases by increasing the temperature and resistance.

The resonance frequency ω_0 is defined by

$$\omega_0^2 = 1/L\,C - R^2/4L^2 \tag{10}$$

where, R, C, and L are the resistance, capacitance, and inductance of the SRR respectively [34]. Here, inductance L is the sum of the superconducting inductance L_s and the geometrical inductance L_G

$$L_G = \mu_0 r \left(\ln \left(\frac{8r}{w + d} \right) - 0.5 \right) \tag{11}$$

Therefore, our metamaterial with structural parameter of $r = 37.5~\mu$m, $w = 5~\mu$m, and $d = 200$ nm gives $L_G = 0.166$ nH [35]. The total capacitance of the BSCCO SRR was obtained from the sum of the gap capacitance $C_g = 0.046$ fF and the surface capacitance $C_s = 0.145$ fF as defined

by the following expressions:

$$C_g = \frac{\varepsilon_0 w d}{g} + \varepsilon_0(w + d + g), \tag{12}$$

$$C_s = \frac{2\varepsilon_0}{\pi}(w + d)\ln(4r/g), \tag{13}$$

$$C = C_g + \alpha C_s \tag{14}$$

where α is the correction factor [35].

To calculate α, we consider the SRR as a perfect electric conductor (PEC), with zero R and L_s, and the resonance frequency $\omega_0^2 = 1/L_G C = 2\pi \times 0.601$ THz. Due to the frequency dependent of the surface impedance, we used a mean impedance value for each temperature which this value is satisfied for $\omega = 2\pi \times 0.5$ THz.

The calculated resonance frequency of BSCCO metamaterial (from (8)) is plotted in Fig. 6(b) in blue. In this curve, we see a red-shift in the resonance frequency of metamaterial below T_c, a blue-shift at T around and just above T_c, and finally a red-shift again at T far from T_c. The theoretical result shows the same tuning trend as the simulation result (red) does. Since we did not observe any resonances above 100 K in simulation, no corresponding data is specified so the second red-shift is not seen in the red graph.

From simulation results, we obtain the relative frequency tuning of BSCCO metamaterial ($f_{max} - f_{min})/f_{max} \approx 7\%$, where f_{max} and f_{min} are the resonance frequency maximum and minimum. This is comparable to the frequency tuning of a YBCO metamaterial with a thickness of 180 nm [34].

The resonance quality factor Q is shown in the inset of Fig. 6(b). Here, $Q = f/\Delta f$ is defined as the ratio of the resonance frequency f to the full width at half maximum (FWHM) of the resonance Δf. By increasing T, the resonance linewidth increases so Q decreases. The resonance completely damps at above $T = 100$ K where Q becomes zero. At 10 K our BSCCO metamaterial has a resonance with $Q = 6.47$. This is comparable to gold (Au) THz metamaterials with the same thickness and geometrical dimensions (not shown here). However, Au metamaterial resonance strength and frequency tuning are much less T- dependent in comparison to high-T_c superconductors [36].

3. Conclusion

We proposed the first BSCCO SRRs and investigated the effect of temperature on resonance properties of metamaterial by numerical simulation and theoretical calculations. We showed that a proper designed BSCCO SRRs could result in the transmission resonances with frequency tunability and quality factor as good as YBCO and Au THz metamaterials. Our results suggest that the proposed metamaterial can be integrated with the IJJ THz emitters to fulfill some of their challenging open issues and to improve their functionalities such as tuning the emission frequency, controlling the emission polarization and directivity, and output power enhancement.

References

[1] R. Singh and N. Zheludev, "Materials: Superconductor photonics," *Nature Photon.*, vol. 8, no. 9, pp. 679—680, Sep. 2014.
[2] S. Savel'ev, V. Yampol, and F. Nori, "Surface Josephson plasma waves in layered superconductors," *Phys. Rev. Lett.*, vol. 95, no. 18, Oct. 2005, Art. no. 187002.
[3] A. L. Rakhmanov, V. A. YampolSkii, J. A. Fan, F. Capasso, and F. Nori, "Layered superconductors as negative refractive index metamaterials," *Phys. Rev. B—Condens. Matter Mater. Phys.*, vol. 81, no. 7, pp. 3–8, Feb. 2010.
[4] A. Tsiatmas *et al.*, "Superconducting plasmonics and extraordinary transmission," *Appl. Phys. Lett.*, vol. 97, no. 11, Sep. 2010, Art. no. 11110.
[5] Z. Tian *et al.*, "Terahertz superconducting plasmonic hole array.," *Opt. Lett.*, vol. 35, no. 21, pp. 3586–3588, Nov. 2010.
[6] V. A. Fedotov *et al.*, "Temperature control of Fano resonances and transmission in superconducting metamaterials," *Opt. Exp.*, vol. 18, no. 9, pp. 9015–9019, Apr. 2010.
[7] N. K. Grady *et al.*, "Nonlinear high-temperature superconducting terahertz metamaterials," *New J. Phys.*, vol. 15, Oct. 2013, Art. no. 105016.

[8]   G. R. Keiser, J. Zhang, X. Zhao, X. Zhang, and R. D. Averitt, "Terahertz saturable absorption in superconducting metamaterials," *J. Opt. Soc. Amer. B*, vol. 33, no. 12, pp. 2649–2655, Nov. 2016.

[9]   S. F. Lee *et al.*, "a-b Plane microwave surface impedance of a high-quality $Bi_2Sr_2CaCu_2O_{8+\delta}$ single crystal," *Phys. Rev. Lett.*, vol. 77, no. 4, pp. 735–738, Jul. 1996.

[10] C. C. Homes, T. Timusk, R. Liang, D. A. Bonn, and W. N. Hardy, "Optical conductivity of c-axis oriented $YBa_2Cu_3O_{6.70}$, evidence for a pseudogap" *Phys. Rev. Lett.*, vol. 71, pp. 1645–1648, Sep. 1993.

[11] K. Delfanazari *et al.*, "Effect of bias electrode position on terahertz radiation from pentagonal mesas of superconducting $Bi_2Sr_2CaCu_2O_{8+\delta}$," *IEEE Trans. THz Sci. Technol.*, vol. 5, no. 3, pp. 505–511, Feb. 2015.

[12] K. Delfanazari *et al.*, "Terahertz oscillating devices based upon the intrinsic Josephson junctions in a high temperature superconductor," *J. Infrared, Millim., THz Waves*, vol. 35, no. 1, pp. 131–146, Sep. 2014.

[13] U. Welp, K. Kadowaki, and R. Kleiner, "Superconducting emitters of THz radiation," *Nature Photon.*, vol. 7, no. 9, pp. 702–710, Sep. 2013.

[14] R. A. Klemm *et al.*, "Modeling the electromagnetic cavity mode contributions to the THz emission from triangular $Bi_2Sr_2CaCu_2O_{8+\delta}$ mesas," *Phys. C Supercond. Appl.*, vol. 491, pp. 30–34, Jul. 2013.

[15] K. Delfanazari *et al.*, "Study of coherent and continuous terahertz wave emission in equilateral triangular mesas of superconducting $Bi_2Sr_2CaCu_2O_{8+\delta}$ intrinsic Josephson junctions," *Phys. C Supercond. Appl.*, vol. 491, pp. 16–19, Aug. 2013.

[16] D. Y. An *et al.*, "Terahertz emission and detection both based on high-Tc superconductors: Towards an integrated receiver," *Appl. Phys. Lett.*, vol. 102, no. 9, Mar. 2013, Art. no. 92601.

[17] T. Kashiwagi *et al.*, "Efficient fabrication of intrinsic-Josephson-junction terahertz oscillators with greatly reduced self-heating effects," *Phys. Rev. Appl.*, vol. 4, no. 5, Nov. 2015, Art. no. 54018.

[18] T. Kashiwagi *et al.*, "A high-T_c intrinsic Josephson junction emitter tunable from 0.5 to 2.4 terahertz," *Appl. Phys. Lett.*, vol. 107, no. 8, Aug. 2015, Art. no. 082601.

[19] L. Ozyuzer *et al.*, "Terahertz wave emission from intrinsic Josephson junctions in high-T_c superconductors," *Supercond. Sci. Technol.*, vol. 22, no. 11, Oct. 2009, Art. no. 114009.

[20] K. Kadowaki *et al.*, "Evidence for a dual-source mechanism of terahertz radiation from rectangular mesas of single crystalline $Bi_2Sr_2CaCu_2O_{8+\delta}$ intrinsic Josephson junctions," *J. Phys. Soc. Jpn*, vol. 79, no. 2, Feb. 2010, Art. no. 023703.

[21] V. M. Krasnov, "Interlayer tunneling spectroscopy of $Bi_2Sr_2CaCu_2O_{8+\delta}$: A look from inside on the doping phase diagram of high-T_c superconductors," *Phys. Rev. B*, vol. 65, no. 14, Mar. 2002, Art. no. 140504.

[22] J. N. Eckstein and I. Bozovic, "High-temperature superconducting multilayers and heterostructures grown by atomic layer-by-layer molecular beam epitaxy," *Annu. Rev. Mater. Sci.*, vol. 25, no. 1, pp. 679–709, Aug. 1995.

[23] R. Mallozzi, J. Corson, J. Orenstein, J. N. Eckstein, and I. Bozovic, "Terahertz conductivity and c-axis plasma resonance in $Bi_2Sr_2CaCu_2O_{8+\delta}$," *J. Phys. Chem. Solids*, vol. 59, no. 1012, pp. 2095–2099, Oct./Nov. 1998.

[24] S. Tajima, G. D. Gu, S. Miyamoto, A. Odagawa, and N. Koshizuka, "Optical evidence for strong anisotropy in the normal and superconducting states in $Bi_2Sr_2CaCu_2O_{8+z}$," *Phys. Rev. B*, vol. 48, no. 21, pp. 16164–16167, Dec. 1993.

[25] S. V Dordevic *et al.*, "Signatures of bilayer splitting in the c-axis optical conductivity of double layer cuprates," *Phys. Rev. B*, vol. 69, no. 9, Mar. 2004, Art. no. 094511.

[26] Y. Matsuda, M. B. Gaifullin, K. Kumagai, K. Kadowaki, and T. Mochiku, "Collective Josephson plasma resonance in the vortex state of $Bi_2Sr_2CaCu_2O_{8+\delta}$," *Phys. Rev. Lett.*, vol. 75, no. 24, pp. 4512–4515, Dec. 1995.

[27] T. Motohashi, J. Shimoyama, K. Kitazawa, and K. Kishio, "Observation of the Josephson plasma reflectivity edge in the infrared region in Bi-based superconducting cuprates," *Phys. Rev. B*, vol. 61, no. 14, pp. R9269–R9272, Nov. 2000.

[28] H. Murakami, T. Kiwa, M. Tonouchi, T. Uchiyama, I. Iguchi, and Z. Wang, "Time-domain terahertz spectroscopy of $Bi_2Sr_2CaCu_2O_{8+\delta}$ thin film," *Phys. C Supercond.*, vol. 367, no. 1, pp. 322–326, Feb. 2002.

[29] J. Hwang, T. Timusk, and G. D. Gu, "Doping dependent optical properties of $Bi_2Sr_2CaCu_2O_{8+\delta}$," *J. Phys. Condens. Matter*, vol. 19, no. 12, Mar. 2007, Art. no. 125208.

[30] J. Corson, J. Orenstein, S. Oh, J. O'Donnell, and J. N. Eckstein, "Nodal quasiparticle lifetime in the superconducting state of $Bi_2Sr_2CaCu_2O_{8+\delta}$," *Phys. Rev. Lett.*, vol. 85, no. 12, pp. 2569–2572, Sep. 2000.

[31] J. Shan, F. Wang, E. Knoesel, M. Bonn, and T. F. Heinz, "Measurement of the frequency-dependent conductivity in sapphire," *Phys. Rev. Lett.*, vol. 90, no. 24, Jun. 2003, Art. no. 247401.

[32] J. Gu *et al.*, "Terahertz superconductor metamaterial," *Appl. Phys. Lett.*, vol. 97, no. 7, Aug. 2010, Art. no. 71102.

[33] J. Wu *et al.*, "Tuning of superconducting niobium nitride terahertz metamaterials," *Opt. Exp.*, vol. 19, no. 13, pp. 12021–12026, 2011.

[34] H. T. Chen *et al.*, "Tuning the resonance in high-temperature superconducting terahertz metamaterials," *Phys. Rev. Lett.*, vol. 105, no. 24, Dec. 2010, Art. no. 247402.

[35] O. Sydoruk, E. Tatartschuk, E. Shamonina, and L. Solymar, "Analytical formulation for the resonant frequency of split rings," *J. Appl. Phys.*, vol. 105, no. 1, Jan. 2009, Art. no. 14903.

[36] R. Singh *et al.*, "Influence of film thickness in THz active metamaterial devices: A comparison between superconductor and metal split-ring resonators," *Appl. Phys. Lett.*, vol. 103, no. 6, Aug. 2013, Art. no. 61117.